# ANALYSIS OF THE DYNAMIC BEHAVIOR OF AIRCRAFT STRUCTURES DURING CRASH IMPACTS



Gil Wittlin
R&D Engineer
Lockheed Aeronautical Systems Company
2555 North Hollywood Way
Burbank, California 91520

Larry Neri
Program Manager, Structures
Federal Aviation Administration
Technical Center
Atlantic City Airport, NJ 08405

## Abstract

The paper describes digital computer program "KRASH," developed under U.S. Army and Federal Aviation Administration sponsorship for the purpose of performing aircraft crash dynamics analysis. The program predicts the response of vehicles to multidirectional crash environments. The program computes the time histories of N interconnected masses, each allowed six degrees of freedom defined by inertial coordinates $X_i$, $Y_i$, $Z_i$, and Eulerian angles $\phi_i$, $\theta_i$, $\psi_i$, where i = 1, 2...N. Euler's equations of motion are integrated numerically to obtain velocities, displacements, and rotations. Gravity forces, internal forces and moments, and external forces are computed. For small deflections a linear analysis is obtained, and for large deflections general plastic deformation is allowed. The program provides for unloading and subsequent reloading along a linear elastic line.

Program KRASH describes the interaction between a series of massless interconnecting structural elements and concentrated rigid body masses to which the structural elements are attached to their ends with the appropriate end fixity (pinned, fixed, etc.). The interconnecting elements represent the stiffness characteristics of the structure between the masses. The masses can translate and rotate in all directions under the influence of the external forces (i.e., gravity, aerodynamics, impact), as well as the constraining internal element forces. The movement of the masses, consequently, results in changes in the relative distortion of the structural elements and, in turn, results in a new set of element forces acting throughout the system. The manner in which the structure moves and the forces act is directly related to the manner in which the aircraft being analyzed is modeled and the direction and magnitude of the external forces, as is the situation whenever real structure is idealized mathematically.

Yield strength criteria which are not explicitly defined in the program are nonetheless accounted for in program KRASH by a unique feature which introduces and uses stiffness reduction factors (KRs). These factors modify the linear stiffness of each structural element. The actual instantaneous beam stiffness is the product of linear input stiffness and the KR factors. The stiffness reduction factor is used to describe the pre-failure and post-failure load-deflection curve for each structural element, and defines the total load deflection curve which encompasses the yield strength of the structures. The technique is based on the premise that only a portion of the major structural elements need be modeled in detail in the post-failure region.

The paper also discusses many of program KRASH's features, which have evolved over many years of development and usage. The validity of the program as an accepted industry tool has been established for many different aircraft configurations and impact conditions. The damage experienced by the structures to which the program has been applied is highly nonlinear and far ranging. The paper illustrates the types of structure which include rotary-wing, light fixed-wing, and transport category aircraft, as well as narrow-body and wide-body airplane airframe sections. Included in the paper is a description of KRASH validation tests and models, a range of application both for metals and composites, pertinent response time histories and deformations. Of particular interest is the recent application of the program to help establish crash design criteria.

## Introduction

The decade of the 1980s has seen significant progress in application of analytical modeling programs for the assessment of aircraft structural crash dynamics behavior. This is particularly true for rotary-wing aircraft as evidenced by the numerous papers on the subject of analytical modeling presented at the annual meeting of the 1986 American Helicopter Society (AHS) (Reference 1). Program KRASH was the main topic presented in many of the papers at that AHS meeting. The development of program KRASH evolved over a period of time and sequence of applications, aided by numerous planned crash tests of different aircraft configurations and a large independent user community.

At the onset of the 1970s the U.S. Army, Ft. Eustis Directorate, desired an analytical capability to determine helicopter structure

dynamic responses to multidirectional crash impact forces. Thus, the development of program KRASH was initiated. KRASH, often is referred to as a 'hybrid' program because its coding allows the use of experimental data as input. The program also provides for approximate representations of complex, large nonlinear behavior via the use of a set of standard stiffness reduction factors. The uniqueness of the KRASH coding philosophy has provided the aircraft industry an effective analytical tool, particularly for design trade-off studies. Subsequent to the U.S. Army's sponsored efforts (Reference 2), KRASH was upgraded under an FAA contract (Reference 3), and its capability directed toward the analysis of light fixed-wing aircraft subjected to crash impact conditions. Recently completed FAA sponsored research (Reference 4), has resulted in additional program enhancements. This paper describes pertinent features and coding associated with program KRASH. In addition to earlier validation models, the paper presents recent applications to narrow-body jet transport airplanes, as part of a joint FAA/NASA program, involving airframe section drop tests, a full scale airplane ('Laurinburg') drop test and a Controlled Impact Demonstration (CID) test provided the framework by which analytical modeling of the structure dynamic behavior of transport category airplanes in a survivable crash environment could be enhanced, validated and applied. This paper, in addition to showing the KRASH correlation with the CID test, describes post-CID applications of KRASH. In this latter study, the validated KRASH model results in conjunction with airframe section and full-scale airplane test data are used to develop a survivable crash design envelope for transport category aircraft.

## Program KRASH

### General Description

A detailed description of program KRASH theory is provided in Reference 5. The following provides some insight into the methodology contained in the code. Digital computer program KRASH predicts the response of vehicles to multi-directional crash environments. The program computes the time histories of N interconnected masses, each allowed six degrees of freedom defined by inertial coordinates $x_i$, $y_i$, $z_i$ and Eulerian angles $\phi_i$, $\theta_i$, $\psi_i$, where $i = 1, 2...N$. Euler's equations of motion are written for each mass. The equations of motion are integrated numerically to obtain velocities, displacements, and rotations. Gravitational forces, internal forces and moments, and external forces are computed. For small deflections a linear analysis is obtained, and for large deflections general plastic deformation is allowed. The program provides for unloading and subsequent reloading along a linear elastic line.

Program KRASH describes the interaction between a series of massless interconnecting structural elements and concentrated rigid body masses to which the structural elements are attached at their ends with the appropriate and fixity (pimed, fixed). The structural elements can be connected between node points which are offset from and rigidly attached to selected mass points. The interconnecting elements are nonlinear beams which represent the stiffness characteristics of the structure between the masses. The masses can translate and rotate in all directions under the influence of the external forces (i.e., gravity, aerodynamic, impact), as well as the constraining internal beam element forces. The movement of the masses results in changes in the relative distortion of the structural elements and, in turn, results in a new set of element forces acting throughout the system.

Computer Program KRASH has the capability to:

1. Define the response of six degrees of freedom (DOF) at each representative location, including three translations and three rotations.

2. Determine mass accelerations, velocities, and displacements and internal member loads and deformations at each time interval.

3. Provide for general nonlinear stiffness properties in the plastic regime, including different types of load-limiting devices, and determine the amount of permanent deformation.

4. Include structural damping.

5. Determine how and when rupture of an element takes place and redistribute the loading over the remaining structural elements.

6. Provide for ground contact by external structure modeled as nonlinear springs. Sliding friction and a nonrigid ground surface are included.

7. Define mass penetration into an occupiable volume.

8. Define the volume change due to structural deformations of the occupiable volume.

9. Include measures of injury potential to the occupants, including the probability of spinal injury indicated by the Dynamic Response Index (DRI) and the probability of head injury indicated by Severity Index (SI), and Head Impact Criteria (HIC).

10. Determine the distribution of Rinetic and potential energy by mass item, the distribution of strain and damping energy by element, and the crushing and sliding friction energy associated with each external spring.

11. Determine the vehicle response to an initial condition that includes linear and angular velocity about three axes and any arbitrary vehicle attitude.

12. Provide a measure of the airplane velocity, forces and displacements by means of translational momentum relationships.

13. Analyze an impact into a horizontal ground and/or an inclined slope.

14. Provide a measure of the stress state of internal beam elements.

15. Analyze a mathematical model containing up to 80 masses and 150 internal beam elements.

16. Determine the response of the vehicle to user-input accelerations and/or forces at specified mass points.

Program KRASH was developed in three stages, as depicted in Figure 1, under sponsorship of the U.S. Army initially and subsequently the Federal Aviation Administration (FAA). Table 1 denotes many of the program features as well as the stage of development at which feature was incorporated or enhanced.

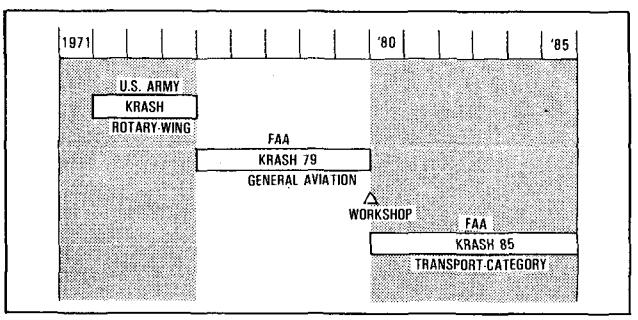


Figure 1. KRASH Development 1971-1985

## Coordinate Systems

Figure 2 depicts a general airplane model. The lumped masses $m_i$, $m_j$, $m_k$ are interconnected by beams ij and jk. Three external springs are shown radiating outward from $m_k$ with end points denoted by $C_{xk}$, $C_{yk}$, and $C_{zk}$. The center of gravity of the airplane (generally does not exist as an explicit mass point) is denoted by G. Several coordinate systems noted in Table 2 were established.

TABLE 1. COMPARISON OF PERTINENT PROGRAM FEATURES

| FEATURES | KRASH | KRASH 79 | KRASH 85 |
|---|---|---|---|
| 1. ENERGY DISTRIBUTION | YES | YES* | YES** |
| 2. ELEMENT RUPTURE | YES | YES* | YES* |
| 3. INJURY CRITERIA (DRI)[a] | YES | YES* | YES |
| 4. PLOT CAPABILITY/SUMMARIES | YES | YES | YES** |
| 5. VOLUME PENETRATION | YES | YES | YES |
| 6. PLASTIC HINGE ALGORITHM | NO | YES | YES* |
| 7. SHOCK STRUT | NO | YES | YES |
| 8. FLEXIBLE AND/OR SLOPED TERRAIN | NO | YES | YES |
| 9. ACCELERATION PULSE EXCITATION | NO | YES | YES |
| 10. UNSYMMETRICAL BEAM REPRESENTATION | NO | YES | YES |
| 11. STANDARD MATERIAL PROPERTIES | NO | YES | YES |
| 12. EXTERNAL SPRING DAMPING | NO | YES | YES |
| 13. MASS LOCATION PLOTS | NO | YES | YES |
| 14. PRE-AND POST-DATA PROCESSING | NO | YES | YES |
| 15. RESTART CAPABILITY | NO | YES | YES |
| 16. SYMMETRICAL MODEL CAPABILITY | NO | YES | YES |
| 17. CG FORCE MOTIONHISTORY | NO | YES | YES* |
| 18. VOLUME CHANGE CALCULATIONS | NO | YES | YES |
| 19. STANDARD NONLINEAR CURVES | NO | 5 | 6 |
| 20. STIFFNESS REDUCTION FEATURE (KRF)[b] APPLICABLE TO DAMPING | NO | NO | YES |
| 21. COMBINED FAILURE LOAD (LIC)[c] | NO | NO | YES |
| 22. INITIAL BALANCE-NASTRAN | NO | NO | YES |
| 23. TIRE VERTICAL SPRING | NO | NO | YES |
| 24. ARBITRARY MASS NUMBERING | NO | NO | YES |
| 25. EXTERNAL FORCE LOADING | NO | NO | YES |
| 26. OLEO METERING PIN | NO | NO | YES |
| 27. ADDITION OF DESCRIPTIVE NAMES TO IDENTIFY INPUT DATA | NO | NO | YES |

*ENHANCED ONE LEVEL. **ENHANCED TWO LEVELS

[a]DYNAMIC RESPONSE INDEX [b]STIFFNESS REDUCTION FACTOR [c]LOAD INTERACTION CURVE

Any quantity which can be expressed as a vector in one coordinate system (forces, moments, displacements, velocities, accelerations, but not large rotations) can be, likewise, specified in another coordinate system by use of an Eulerian transformation matrix relating the two coordinate systems. The various transformation matrices used are summarized in Table 3. The basic sign convention used for all displacements, rotations, velocities, accelerations, forces and moments is that all quantities are positive in the positive direction of the axes shown in Figure 2.

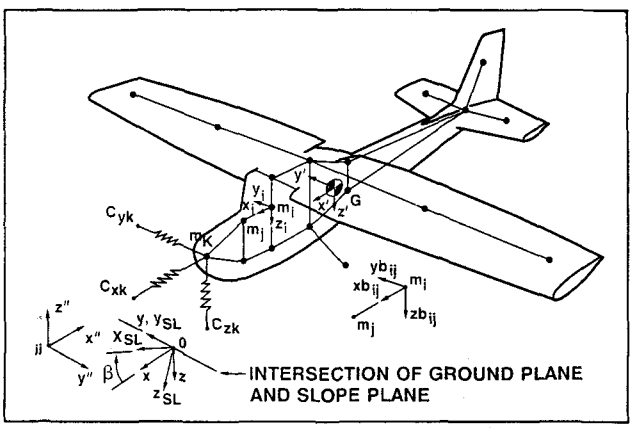


Figure 2. Mathematical Model of Airplane

## Forces

The following forces and moments act on each lumped mass:

- Gravity forces
  The weight acting along the ground fixed $O_Z$ axis transformed into body axes.

- Aerodynamic forces
  Either a constant lift acting on each mass

TABLE 2. COORDINATE SYSTEM DESCRIPTION

| COORDINATE SYSTEM | NOTATION* | ORIGIN LOCATED AT* | DESCRIPTION* |
|---|---|---|---|
| GROUND (R) | Oxyz | 0 | THE xy PLANE (z = 0) CORRESPONDS TO THE GROUND SURFACE. THE GROUND COORDINATE SYSTEM IS CONSIDERED AN INERTIAL COORDINATE SYSTEM FOR WRITING THE DYNAMIC EQUATIONS OF MOTION. |
| SLOPE (R) | $O_{x_{SL}y_{SL}z_{SL}}$ | 0 | THE $x_{SL}$ AXIS IS POSITIVE FORWARD UP THE SLOPE, THE $y_{SL}$ AXIS IS POSITIVE TO THE RIGHT, AND THE $z_{SL}$ AXIS IS POSITIVE PERPENDICULAR TO THE SLOPE, GOING INTO THE SLOPE. THIS COORDINATE SYSTEM IS THE SAME AS THE GROUND COORDINATE SYSTEM, ROTATED THROUGH AN ANGLE BETA (B) POSITIVE CLOCKWISE ABOUT THE Oy GROUND AXIS. THE $O_{x_{SL}y_{SL}}$ PLANE REPRESENTS A PLANE INCLINED AT AN ANGLE BETA WITH RESPECT TO THE HORIZONTAL GROUND PLANE. BETA IS A CONSTANT INPUT ANGLE THAT CAN LIE IN THE RANGE FROM ZERO TO NINETY DEGREES. |
| AIRPLANE (L) | Hx″y″z″ | H | THE ORIGIN, POINT H, CORRESPONDS TO F.S.O., B.L.O., W.L.O. THIS COORDINATE SYSTEM IS USED ONLY TO INPUT THE COORDINATES OF THE LUMPED MASS POINTS, SINCE THE COORDINATES OF THE POINTS ARE USUALLY AVAILABLE IN TERMS OF F.S., B.L., AND W.L. FIXED IN AIRPLANE AXIS. |
| CENTER-OF-GRAVITY (R) | Gx′y′z′ | G | THESE AXES ARE PARALLEL TO THE Hx″y″z″ AXES. |
| BODY (R) | MiXiYiZi | | EACH LUMPED MASS HAS ITS OWN RIGHTHANDED COORDINATE SYSTEM FIXED IN THE MASS. THE INITIAL ORIENTATION OF EACH OF THESE COORDINATE SYSTEMS IS ARBITRARY, AND IT IS SPECIFIED BY MEANS OF THREE INPUT EULER ANGLES FOR EACH MASS, RELATING ITS INITIAL ORIENTATION TO THE Gx′y′z′ CENTER-OF-GRAVITY COORDINATE SYSTEM. THESE ANGLES ARE $\phi_i''$, $\theta_i''$, $\psi_i''$. NORMALLY THE BODY COORDINATE SYSTEM IS TAKEN AS INITIALLY PARALLEL TO THE CENTER-OF-GRAVITY COORDINATE SYSTEM (AND HENCE, THE THREE INPUT EULER ANGLES ARE SET = 0), SINCE THE INERTIAL DATA IS GENERALLY AVAILABLE ABOUT THESE AXES. |
| BEAM (R) | $m_i x b_{ij} y b_{ij} z b_{ij}$ | | THE $xb_{ij}$ AXIS IS ALONG A STRAIGHT LINE FROM $m_i$ TO $m_j$. AS THE MASSES MOVE, THE COORDINATE SYSTEM CHANGES ORIENTATION SO THAT $xb_{ij}$ IS ALWAYS POINTING FROM $m_i$ TO $m_j$. IF THE BEAM CONNECTS NODE POINTS WHICH ARE OFFSET FROM THE MASS POINTS, THE $xb_{ij}$ ALWAYS POINTS FROM THE NODE POINT RIGIDLY ATTACHED TO MASS $m_i$ TO THE NODE POINT RIGIDLY ATTACHED TO MASS $m_j$. THE DIRECTION OF $yb_{ij}$ AND $zb_{ij}$ (THEY ARE MUTUALLY PERPENDICULAR) IS ARBITRARY AND IS DEFINED INTERNALLY WITHIN THE PROGRAM. EACH BEAM ij HAS A BEAM COORDINATE SYSTEM USED TO COMPUTE THE BEAM FORCES AND MOMENTS. |
| AERODYNAMIC (R) | $m_i x_{ai}$ $y_{ai}$ $z_{ai}$ | $m_i$ | THIS IS A RIGHT-HANDED COORDINATE SYSTEM WITH ORIGIN AT $m_i$. THE $m_i x_{ai}$ AXIS POINTS IN THE DIRECTION OF THE PROJECTION OF THE RELATIVE WIND ON THE $m_i x_i z_i$ PLANE OF MASS i, AND IS INCLINED AT AN ANGLE OF ATTACK $\alpha$ NOSE DOWN FROM THE BODY FIXED AXIS $m_i x_i$. THE $m_i y_{ai}$ AXIS IS PARALLEL TO $m_i y_i$. THE AERODYNAMIC COORDINATE SYSTEM RESULTS FROM ROTATING THE ENTIRE BODY COORDINATE SYSTEM $m_i x_i y_i z_i$ THROUGH AN ANGLE $\alpha$, NOSE DOWN, ABOUT THE $m_i y_i$ AXIS. THE TIME-VARYING AERODYNAMIC LOADS ARE CALCULATED IN THE AERODYNAMIC COORDINATE SYSTEM. |

(R) DENOTES RIGHT-HANDED COORDINATE SYSTEM; x IS POSITIVE FORWARD, y POSITIVE RIGHT, z POSITIVE DOWN

(L) DENOTES LEFT-HANDED COORDINATE SYSTEM; x IS POSITIVE AFT, y POSITIVE LEFT, z POSITIVE UPWARD

* REFERS TO FIGURE 2

specified by the user or time varying forces and moments in all six directions. The latter employs conventional steady state aerodynamics utilizing stability derivatives.

- Externally applied forces and accelerations
  Optional time history forces or accelerations at selected mass points.

- Internal forces and moments
  Resulting from deformations of the interconnecting beams as the lumped masses move. For each mass the contribution from the various beams that attach to that mass are summed. All the internal strain from calculations are performed on an incremental basis. However, damping forces are total, not incremental based on current beam end velocities.

TABLE 3. TRANSFORMATION MATRICES

| MATRIX | TRANSFORMS FROM | TO | USING ANGLES | ANGLES CONSTANT OR VARYING |
|---|---|---|---|---|
| $[A_i]$ | ith BODY AXES | GROUND AXES | $\phi_i, \theta_i, \psi_i$ | VARYING |
| $[A_{ij}]$ | BEAM ij AXES | GROUND AXES | $\phi_{ij}, \theta_{ij}, \psi_{ij}$ | VARYING |
| $[A_i'']$ | ith BODY AXES | cg AXES | $\phi_i'', \theta_i'', \psi_i''$ | CONSTANT |
| $[A']$ | cg AXES | GROUND AXES | $\phi', \theta', \psi'$ | CONSTANT |
| $[A_\beta]$ | cg AXES | GROUND AXES | 0, $\beta$, 0 | CONSTANT |
| $[A_{ai}]$ | AERODYNAMIC AXES | BODY AXES | 0, $\alpha$, 0 | VARYING |

Internal force and moment calculations take into account beam end fixity such as fixed-fixed, pinned-pinned or fixed-pinned. The incremental beam load formulation lends itself readily to plastic hinge modeling. A plastic hinge is treated as a normal linear fixed beam until a defined hinge moment is exceeded. Once the linear moment is equal to the defined plastic hinge moment, the incremental loads are calculated based on the appropriate pinned-end conditions. In terms of incremental beam loads, a plastic hinge corresponds to a pinned joint. Therefore, the time-varying total beam moment remains equal to the defined plastic hinged moment.

Unloading and subsequent reloading invoke fixed end condition coding, and cyclic loading leads to hysteresis loops such as shown in Figure 3. During the constant load portions of Figure 3, pinned-end coding is in effect for calculating incremental loads. For the sloped, varying load regions of Figure 3, fixed-end coding is used for the incremental loads. KR factors are not used in any way for plastic hinge coding. Since the incremental force calculations are always

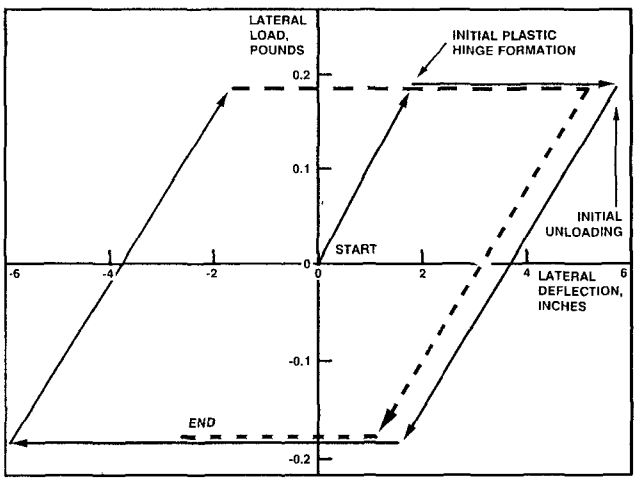


Figure 3. Formation of Hysteresis Loops for Lateral Bending of Plastic Hinge Elements

rigorously correct with this formulation, the resulting total load-stroke behavior cannot develop negative strain energy.

Nonlinear Strain Forces and Moments

Figure 4 illustrates a typical nonlinear load-deflection characteristic curve, in this case the axial load at point j, $Fx_j$, versus the axial deflection of j with respect to i, vx. Program KRASH utilizes a piecewise linear representation of the load-deflection curve. At each increment in time, a linear incremental force $dFx_j$ is calculated. This incremental force is then multiplied by a stiffness reduction factor, $KR_x$, to obtain the nonlinear incremental force $dF'_x$. These increments are then summed over time to form the total force $F'x_j$. Figure 5 illustrates a typical incremental deflection dvx, the corresponding linear incremental force $dFx_j$ and the final nonlinear incremental force $dFx_j$.

The stiffness reduction factor $KR_x$ is an input tabular function of deflection vx. Figure 5 shows the $KR_x$ versus vx curve that corresponds to the load-deflection curve in Figure 4. $KR_x$ is just the first derivative of the load-deflection curve with respect to deflection. Any KR curve can be input by the program user to model any general nonlinear behavior. Certain standard curves are available to represent the more common types of nonlinearities. Separate KR tables are input for each of the six directions for which it is desired to model nonlinear behavior, for beam ij. In practice, perhaps only 20 percent or less of all the beams will be modeled nonlinearly. (If no KR table is input, KR = 1 and the beam is linear for the entire run.)

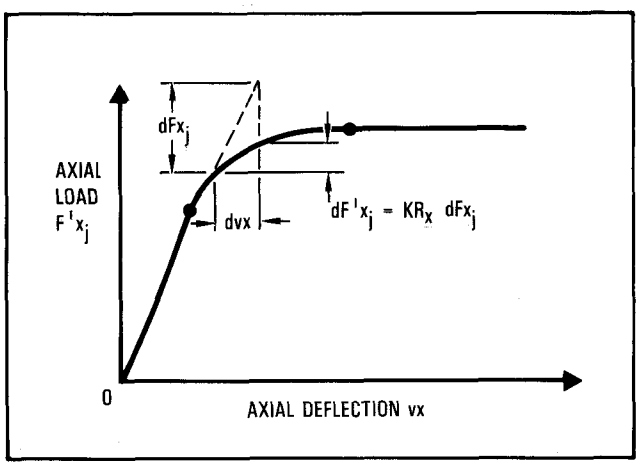


Figure 4. Nonlinear Load Deflection Curve

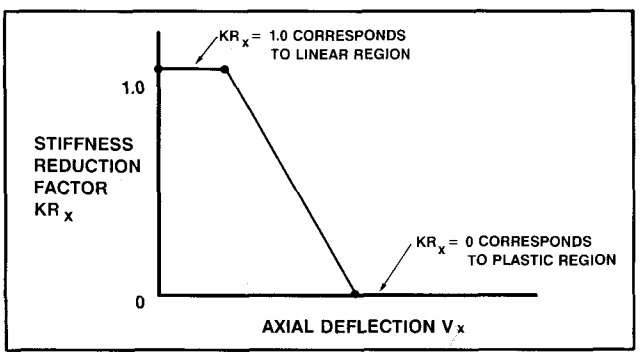


Figure 5. Stiffness Reduction Factor Curve

The program is coded in the following manner. For the coupled degrees of freedom, the direction which goes nonlinear first determines the nonlinear behavior for both coupled directions. This means that if $KR_z$ departs from 1 (linear) before $KR_\Theta$ does, then $KR_z$ is used for the dFz' and $dM\Theta'$ for the remainder of the run. If $KR_\Theta$ goes nonlinear first, then it is used in calculating both dFz' and $dM\Theta'$ for the rest of the run. This analytical model preserves the proportionality that exists between dFz and $dM\Theta$ in the linear system, since the linear incremental forces are always multiplied by the same KR factor. The coupled degrees of freedom y and $\psi$ are treated in the same manner. In each case, both deflection and rotation KR curves are input, even though only one will be used, because it is not known in advance which direction will predominate. Axial and torsional deflections are uncoupled and each has its own KR curve, applicable for the entire analysis.

In addition to the nonlinear load capability just described, the program also allows for unloading and subsequent reloading to proceed along an elastic line. This is illustrated in Figure 6. The ordinate Fk is the total (over time) k-direction load for beam ij. Similarly, $v_k$ is the corresponding total (over time) k-direction deflection.

Without unloading, a typical nonlinear load-stroke curve O-A-B-C-D would occur. If the system unloads at point B, then unloading proceeds until point E is reached. The load at point E is equal in magnitude to that at point B. The slope of B-E is the same as the slope of O-A, and corresponds to

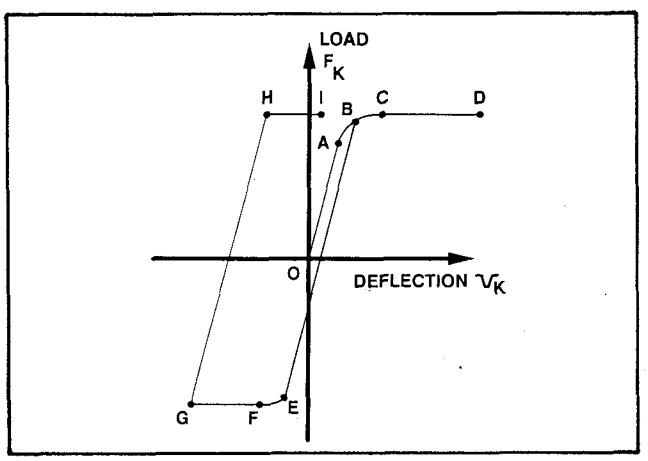


Figure 6. Loading-Unloading Model

$KR_k = 1$. If reloading occurs before point E is reached, then reloading proceeds back to point B, then B-C-D.

If unloading continues beyond point E, then the original nonlinear characteristic curve is resumed. Unloading proceeds along E-F-G, which has the same curve shape as the original B-C-D. Load F-G has the same magnitude as load C-D. In Figure 6, reloading occurs at point G, again along an elastic ($KR_k = 1$) line until point H, with load magnitude equal to G, is reached.

Loading from H to I is a resumption of the original nonlinear behavior, which for the example shown corresponds to $KR_k = 0$. The cyclic hysteretic loading-unloading-reloading can repeat indefinitely.

The important feature represented here is the energy absorbed by the structure in a loading-unloading-reloading cycle such as O-B-E-G-H-I. It is felt that under the large deformation crash conditions that this program is intended to investigate, this energy absorption is far more significant than the small structural damping generally present.

Integration Routine. The equations of motion are integrated numerically in computer program KRASH. The integration scheme employed is a modified predictor-corrector method. Figure 7 shows a time history of a typical response quantity, say u. Assume that u and $\dot{u}$ are known at time t and all previous times. The predicted value of u at $t + \Delta t$, $u_{p_{t+\Delta t}}$ is computed as

$$u_{p_{t+\Delta t}} = u_{t-\Delta t} + 2\Delta t \dot{u}_t$$

This is shown in Figure 7 by the upper dashed line of slope $\dot{u}_t$. Using this predicted value of u at $t + \Delta t$, the derivative u at $t + \Delta t$ is computed from Euler's equations of motion. This derivative is then averaged with u at t to determine a corrected value of u at $t + \Delta t$:

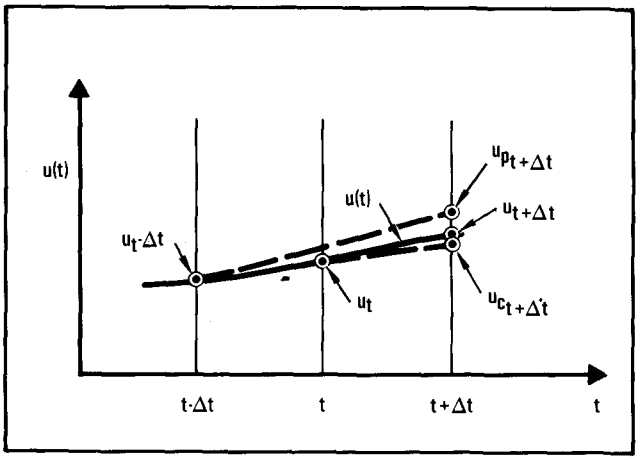


Figure 7. Numerical Integration Scheme

$$u_{c_{t+\Delta t}} = u_t + \frac{\Delta t}{2}(\dot{u}_{t+\Delta t} + \dot{u}_t)$$

This is shown by the lower dashed line in Figure 7. The final value used for $u_{t+\Delta t}$ is a weighted average of the predicted and corrected values. For the present program, the weighting used is 4 to 1 in favor of the corrected value. Hence:

$$u_{t+\Delta t} = 0.8u_{c_{t+\Delta t}} + 0.2u_{p_{t+\Delta t}}$$

Auxiliary Calculations. The program provides output to aid the user in interpreting the dynamic impact event. These data are considered auxiliary calculations since they are not coupled into the equations of motion, and thus do not influence the time history responses. The following is a brief description of some of these parameters.

- Filtered Accelerations
  In order to facilitate comparisons of KRASH analytical results with test results, the program employs a simple first order log filter. The characteristics of the filter are shown in Figure 8.

- Energy Balance Equations
  The primary objective of a crash analysis in the preliminary design phase is to determine how to absorb the initial vehicle kinetic energy while maintaining a livable environment for the occupants.

This task is greatly facilitated if information regarding the spatial distribution of the energy glow through the vehicle is available. With this objective in mind, energy balance equations are developed. These equations do not alter the previously described computations procedures; they merely provide additional information to assist in understanding how the initial kinetic energy is absorbed.

The total system energy at any time is given by the following expression:

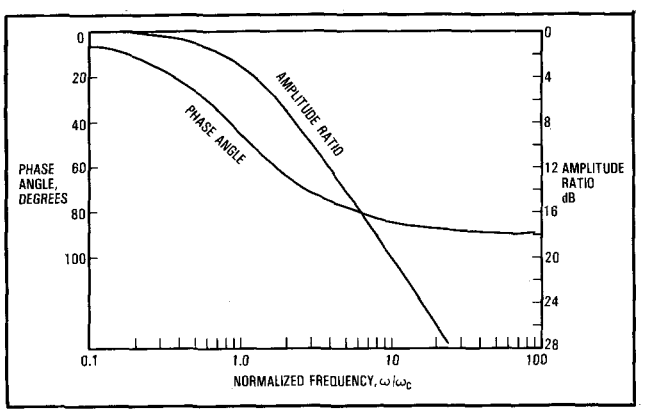


Figure 8. First Order Filter Response Characteristics

$$E_{TOT} = KE + PE + SE + DE + CE + FE - EW$$

where:

$E_{TOT}$ = Total system
KE = Total kinetic energy
PE = Total potential energy
SE = Total strain energy absorbed
DE = Total damping energy dissipated
CE = Total crushing (external spring) energy absorbed
FE = Total friction energy dissipated by sliding of external springs on the ground
EW = Total external work due to external applied forces, accelerations and lifts

The total system energy $E_{TOT}$ remains constant during the analysis. The total kinetic and potential energies result from summing the energies for each mass over the number of masses. The total strain and damping energies are obtained by summing the strain and damping energy for each internal beam element over the number of beams. Crushing and friction energies are the summation of incremental energy changes associated with each spring. The external work accounts for the energy due to applied forces, defined mass accelerations and aerodynamic forces.

- Overall Vehicle Center-of-Gravity Motion
  This calculation determines overall vehicle c.g. force, displacement, acceleration and velocity time history. It is extremely useful in determining representative section load-deflection curves.

- Internal Beam Load Interaction Curve
  Provides a cross plot of any two of the six internal beam loads at a given section, e.g., a plot of beam bending moment versus shear. The program compares the calculated load to the allowable envelope and can initiate rupture if the user elects such an option.

- Human Tolerance Calculations
  Program KRASH includes the capability to estimate the severity of a crash event in terms of the dynamic response of occupants, and the tolerance of the human body to withstand such responses. Analyses available in KRASH are:

  1. Spinal Compression
  2. Head Injury

A measure of spinal injury potential is obtained through Dynamic Response Index (DRI) calculation. The DRI is a nondimensionalized measure of the compression of the human spinal column and statistical data is available relating DRI to the probability of injury.

Head injury potential due to impacting a surface is calculated two ways in a later KRASH version; Head Injury Criteria (HIC) and Severity Index (SI). The program allows the user to save velocity data for subsequent acceleration calculations which are performed in KRASH. Alternatively, the user can input a specified velocity along with the nonlinear load-deflection characteristics of the impacted surface and the program computes the HIC and SI. The respective calculations are:

$$SI = \int_{t_o}^{t_f} a(t)^{2.5}\, dt$$

$$HIC = \left\{ (t_2-t_1) \left[ \frac{1}{(t_2-t_1)} \int_{t_1}^{t_2} a(t)dt \right]^{2.5} \right\}$$

where:

a(t) is the time history of the head acceleration in g's

$t_o$ and $t_f$ are the start end times of the head acceleration time history

$t_2-t_1$ is the head acceleration time increment which is normally $\leq .050$ seconds

## 'KRASH' Aircraft Simulation and Validation

Computer program KRASH has had substantial experimental verification as can be noted from the summary provided in Table 4. The following sections discuss some of the models, test conditions and comparative results for a range of aircraft configurations.

TABLE 4. KRASH EXPERIMENTAL VERIFICATION

| AIRCRAFT | GROSS WEIGHT (Kg) | IMPACT VELOCITY (M/SEC) | | |
|---|---|---|---|---|
| | | VERTICAL | LONGITUDINAL | LATERAL |
| ROTARY WING | | | | |
| UTILITY TYPE | 3909 | 7.0 | – | 5.8 |
| CARGO TYPE | 11045 | 12.8 | 8.3 | – |
| MULTI-PURPOSE | 1727 | 6.0 | 6.0 | – |
| MULTI-PURPOSE | 1645 | 10.0 | – | – |
| COMPOSITE SUBSTRUCTURE | 1605 | 9.1 | – | – |
| COMPOSITE SUBSTRUCTURE | 1605 | 8.8 | – | 3.1 |
| COMPOSITE (ACAP) | 3512 | 12.3 | – | – |
| COMPOSITE (ACAP) | 3421 | 13.3 | 8.5 | – |
| LIGHT-FIXED-WING | | | | |
| SINGLE-ENGINE, HIGH-WING | 1091 | 14.0 | 21.3 | – |
| SINGLE-ENGINE, HIGH-WING | 1091 | 6.7 | 21.7 | – |
| SINGLE-ENGINE, HIGH-WING | 1091 | 14.9 | 21.3 | – |
| SINGLE-ENGINE, HIGH-WING* | 1091 | 13.1 | 21.2 | – |
| TWIN-ENGINE, LOW-WING SUBSTRUCTURE | 248 | 8.4 | – | – |
| TRANSPORT | | | | |
| MEDIUM SIZE* | 72272 | 5.5 | 52.4 | – |
| MEDIUM SIZE | 88636 | 5.3 | 79.2 | – |

Rotary-Wing Aircraft

The initial correlation for KRASH was based on comparisons of analytical results for a combined vertical (23 ft/sec) and lateral impact (18.5 ft/sec). Full-scale crash test of a utility type helicopter. Figure 9 (Reference 2) shows the post-impact configuration for this test. The 31 mass, 37 beam math model for the helicopter crash test, is shown in Figure 10. A comparison of analysis and test results is shown in Figures 11 and 12.

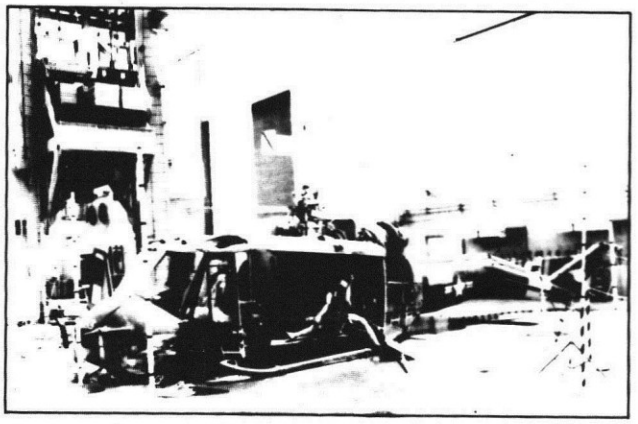

Figure 9. Post-Test Damage, UH-1H Helicopter Crash Test

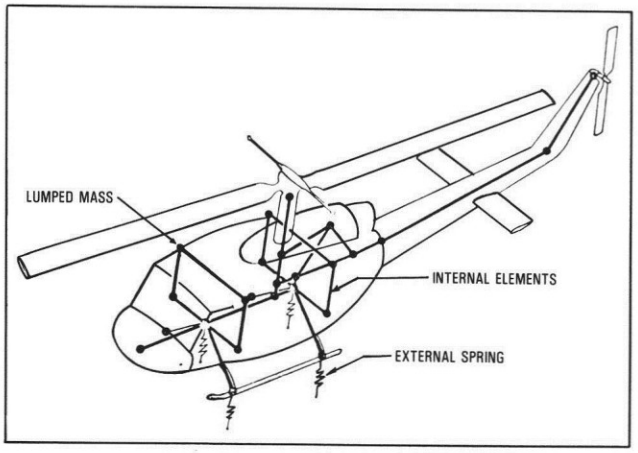


Figure 10. Helicopter Analytical Model

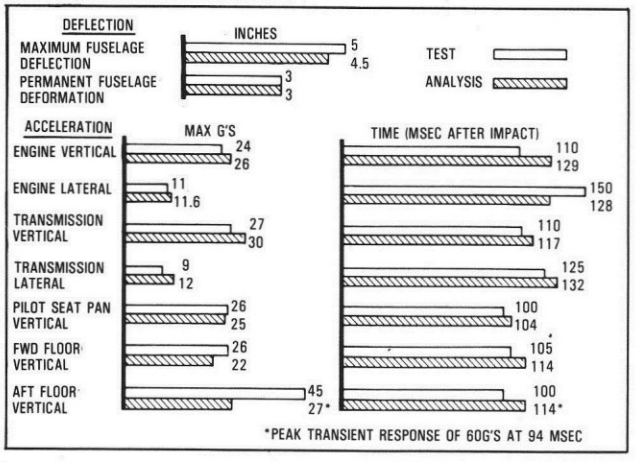


Figure 11. Comparison of Helicopter Crash Test and Analysis Results

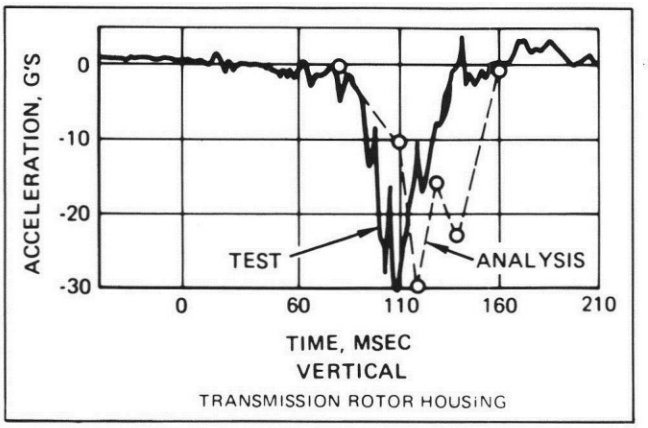


Figure 12. Comparison of Helicopter Acceleration Measured and Analytical Data

Light-Fixed Wing Aircraft

During the mid to late 1970s the FAA sponsored an effort to update KRASH for application to light fixed-wing aircraft. The original KRASH version developed for rotary wing aircraft crash impact analyses was retained and enhanced with the incorporation of additional features. Several comprehensive supporting documents were issued in conjunction with this KRASH release, including a theory volume, a User's Manual and a Programmer's Manual (Reference 6). In support of the updated program four tests of a light fixed-wing aircraft configuration were performed. Figure 13 shows the post-impact configurations for the four full-scale crash tests of a single-engine high-wing general aviation aircraft type. The test conditions for these four tests are shown in Table 5. The single symmetrical KRASH model used for all four tests shown in Figure 14 contained 30 masses and 59 beams. A full airplane model version contained 48

TABLE 5. SUMMARY OF SINGLE-ENGINE, HIGH-WING AIRPLANE CRASH TEST IMPACT CONDITIONS

| | TEST NUMBER | | | |
|---|---|---|---|---|
| | 1 | 2 | 3 | 4 |
| IMPACT VELOCITIES (MPH) | | | | |
| ALONG FLIGHT PATH | 55.5 | 50.8 | 58.1 | 55.9 |
| LONGITUDINAL | 47.4 | 48.6 | 47.6 | 48.4 |
| VERTICAL | 28.7 | 14.8 | 33.2 | 31.9 |
| ANGLES (DEGREES) | | | | |
| FLIGHT PATH($\gamma$) | -30.72 | -17.0 | -34.86 | -32.0 |
| IMPACT ($\theta$) | -30.17 | 13.5 | -39.4 | -34.8 |
| ATTACK ($\alpha$) | 0.57 | +30.5 | -4.54 | -2.8 |
| ROLL ($\phi$) | +4.13 | +3.25 | +18.75 | < 1.0 |
| YAW ($\psi$) | -3.27 | -11.5 | -7.9 | < 1.0 |
| ROTATIONAL VELOCITIES (DEG/SEC) | | | | |
| PITCH ($\dot{\theta}$) | 46.4 | 6.9 | 14.3 | 18.2 |
| ROLL ($\dot{\phi}$) | NEGLIGIBLE | NEGLIGIBLE | NEGLIGIBLE | NEGLIGIBLE |
| YAW ($\dot{\psi}$) | NEGLIGIBLE | NEGLIGIBLE | NEGLIGIBLE | NEGLIGIBLE |

$\gamma$ IS NEGATIVE IN DIVE
$\theta, \dot{\theta}$ ARE POSITIVE NOSE UP RELATIVE TO FLIGHT PATH
$\alpha$ IS POSITIVE NOSE UP RELATIVE TO FLIGHT PATH
$\phi, \dot{\phi}$ ARE POSITIVE RIGHT WING DOWN
$\psi, \dot{\psi}$ ARE POSITIVE TAIL LEFT
AND $\theta = \gamma + \alpha$
FT/SEC = 1.467 x MPH

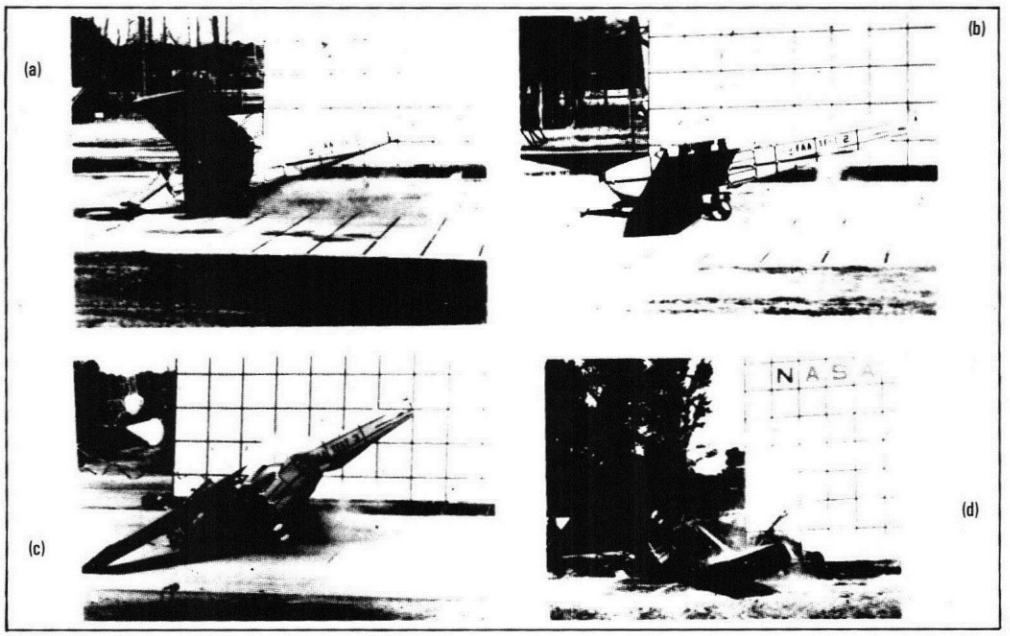


Figure 13. Post-Test Damage, Single-Engine High-Wing Airplane Crash Tests

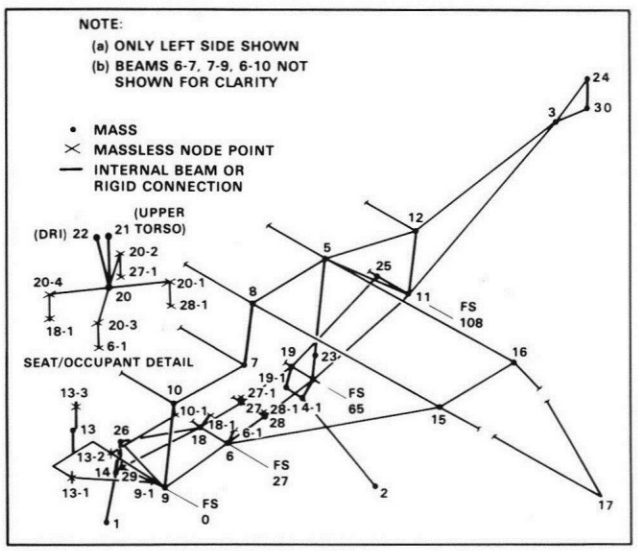


Figure 14. Single-Engine High-Wing Airplane Analytical Model

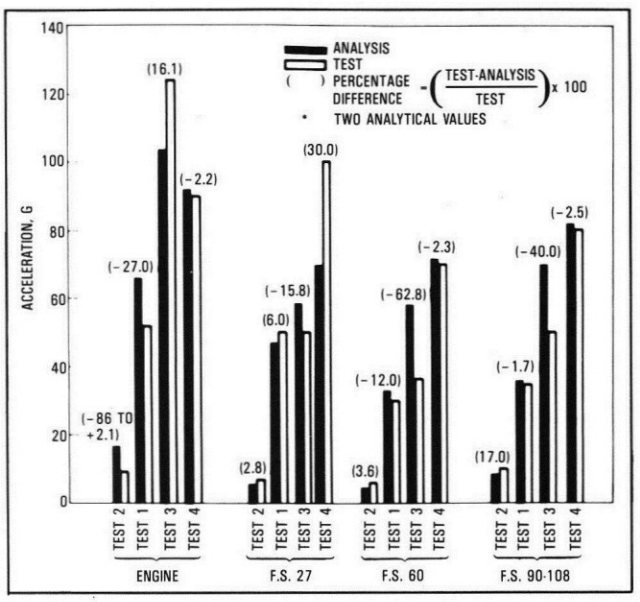


Figure 15. Single-Engine High-Wing Airplane Analysis and Test Vertical Responses

masses and 100 beams. A comparison of analysis and test results is shown in Figures 15 and 16. A detailed description of this effort is provided in Reference 3.

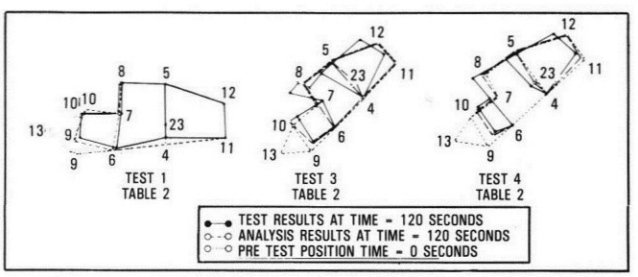


Figure 16. Comparison of Cabin Deformation Single-Engine High-Wing Airplane

## Transport Category Airplanes

A third phase in the development of KRASH occurred during the early 1980s and culminated in a released version denoted KRASH85. The major emphasis of this effort was the development of improved methodology for determining the structural dynamic responses for large transport aircraft in impact survivable crashes. As a prelude to KRASH modifications the major domestic manufacturers of transport aircraft reviewed the accident records for the period 1964-1979 (References 7, 8, 9) and formulated crash

scenarios. Subsequent to this review the FAA and NASA conducted a series of airframe section impact tests (References 10, 11, 12, 13), as well as a full-airplane drop test referred to as the 'Laurinburg' test. These tests were performed in support of full-scale remotely piloted Controlled Impact Demonstration (CID) test (Reference 14). Prior to the pre-CID predictions, the program was used to model the frame section tests and evolve lower fuselage crush springs representative of the frame sections. Figure 17 shows the post-test view of two narrow-body airplane frame section tests, with and without subfloor cargo loading. Force versus displacement curves were developed which were useful in the development of lower fuselage crush characteristics for input into KRASH CID models. Two KRASH models were developed for the CID test. The 24 mass, 23 beam element stick model (Figure 18) and the 48 mass, 137 beam expanded model (Figure 19). The stick model is for the purpose of obtaining overall airframe response and assessing airframe structural integrity and floor accelerations. The expanded model is designed to evaluate detail response.

The Controlled Impact Demonstration test was performed on December 1, 1984, at the NASA Dryden Dry Lake Bed, Edwards Air Force Base, California. The planned impact conditions are compared to the actual impact conditions in Table 6. The CID crash from initial wing contact to subsequent fuselage impact is shown in Figure 20. The test aircraft was in an unplanned roll and yaw to the left attitude just prior to initial ground contact. Subsequently, the aircraft impacted on the left wing outboard No. 1 engine, rotated onto the No. 2 engine and impacted the forward fuselage about 400 msec after the No. 1 engine contact. Peak ground impact responses were developed within 500 msec after initial fuselage ground impact and prior to contact with any ground obstructions. Accordingly, all of the analytical efforts discussed herein deal only with the initial ground impact.

The comparison of analysis results with CID test data was performed for two conditions using the stick model;

- Partial Sequence. - Symmetrical impact on forward fuselage at a reduced sink speed 14 ft/sec (4.27 m/sec), -2° nose down, 0° roll and yaw.

- Complete Sequence. - Unsymmetrical impact on left wing engine No. 1, initial sink speed 17.3 ft/sec (5.27 m/sec), +1° nose up, 13° roll and yaw.

The primary emphasis of the analysis was to determine cabin floor responses which were then used to evaluate dynamic seat testing criteria. A comparison of results of the unsymmetrical impact

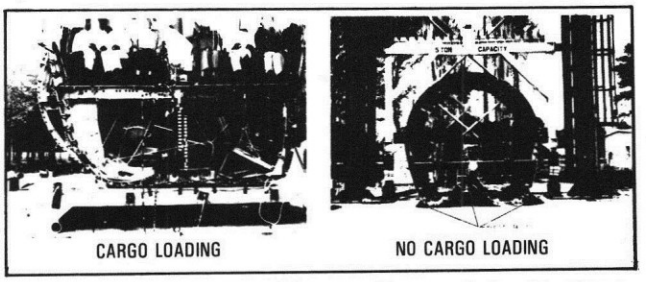


Figure 17. Post-Test Views - Narrow-Body Airplane Fuselage Section Tests

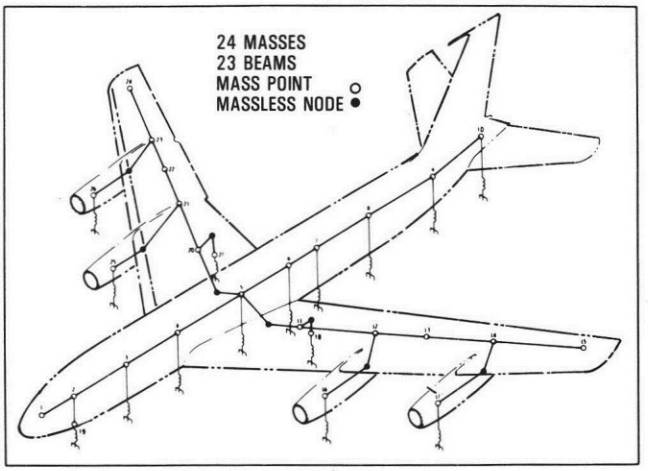


Figure 18. CID Stick Model

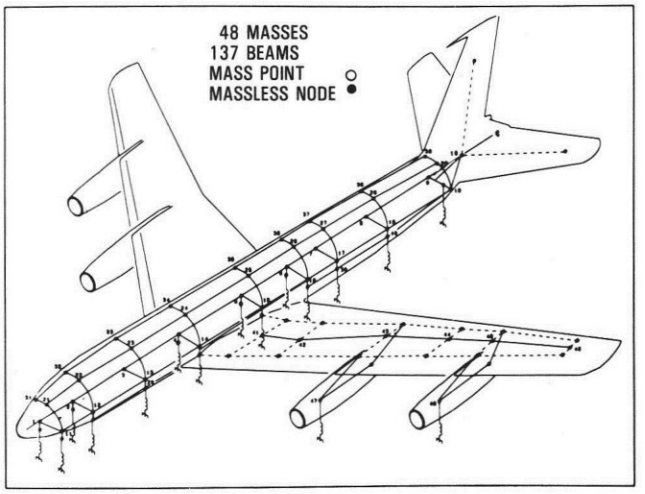


Figure 19. CID Expanded Model

TABLE 6. COMPARISON OF CID PLANNED AND ACTUAL TEST CONDITIONS

| | PLANNED | ACTUAL* |
|---|---|---|
| SINK RATE, FT/SEC | 17 $^{+3}_{-2}$ | 17.3 |
| GROSS WEIGHT, LB | 175 – 195,000 | 192,383 |
| GLIDE PATH, DEGREES | 3.3 TO 4.0 | 3.5 |
| ATTITUDE, DEGREES | 1 ± 1 (NOSE UP) | 0 |
| LONGITUDINAL VELOCITY, KNTS | 150 ± 5 | 151.5 |
| ROLL DEGREES | 0 ± 1 | -13** |
| YAW DEGREES | 0 ± 1 | -13*** |

*IMPACTED ON LEFT WING OUTBOARD ENGINE. INITIAL CONTACT ON FUSELAGE WAS AT FOLLOWING CONDITIONS: 14 FT/SEC SINK SPEED, NOSE-DOWN ATTITUDE (0.-2.0 DEGREES), FORWARD VELOCITY 150 KNTS CONTACTED FUSELAGE (BS 360 – 460) REGION.

**LEFT WING DOWN
***NOSE LEFT

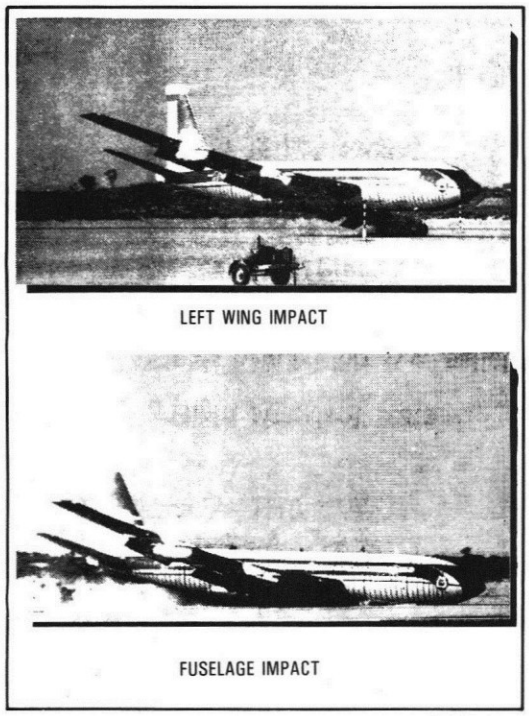


Figure 20. CID Impact on Left Wing and Fuselage

sequence; analysis versus test is provided in Table 7. A comparison of the peak vertical accelerations on the fuselage are provided in Figures 21 and 22.

Considering the unsymmetrical case, the initial impact on the Number 1 engine does not produce significant fuselage responses. As the aircraft settles down and impacts the forward portion of the fuselage the impact forces increase significantly. Thus fuselage impact results in greater impact forces and for this reason the previous condition was considered a symmetrical fuselage impact.

In addition to the peak vertical acceleration comparisons, the correlation between CID modeling and test results included comparisons of:

- Lateral and longitudinal direction accelerations
- Moment distributions along the fuselage and wing

The CID related analytical effort is reported in a series of three reports chronicling the pre-CID study, correlation and post-CID analysis, References 15, 16, and 17.

## Applications

Program KRASH has been used for numerous studies involving a myriad of purposes (References 18 to 26). Included are the following:

- Showing compliance with crash design requirements, e.g., MIL-STD-1290
- Developing crash design criteria

TABLE 7. COMPARISON OF UNSYMMETRICAL IMPACT SEQUENCE; ANALYSIS VERSUS TEST

| | ANALYSIS RESULTS | TEST DATA |
|---|---|---|
| INITIAL FUSELAGE CONTACT | | |
| MASS NO. | 2 | 2-3 |
| TIME (SEC)(1) | 0.432 | 0.400 |
| FUSELAGE CONTACT VELOCITY, M/SEC | 4.19 | 4.27 |
| ENGINE NO. 2 CONTACT | | |
| TIME (SEC)(1) | 0.083 | 0.080 |

(1) AFTER ENGINE NO. 1 INITIAL GROUND CONTACT

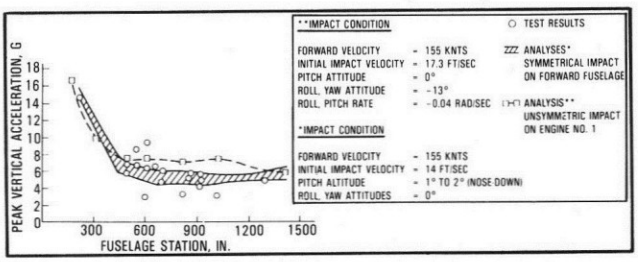


Figure 21. - CID Fuselage Accelerations; Test Versus Analysis

- Modeling composite fuselage structure
- Assessing the use of advanced composite materials in transport airplane lower fuselage design
- Determining incremental weight increase versus crashworthiness level tradeoff
- Performing landing gear simulation
- Modeling occupant/seat systems
- Evaluating car-barrier impacts

The following discussion provides some insight into two of the above-noted areas; namely crash design criteria and composites.

Crash Design Requirements. KRASH has been applied by numerous aircraft manufacturers to evaluate a wide range of design configurations. Several studies (References 18, 19, 20), have been performed in which KRASH was used to help show compliance with severe crash impacts specified in MIL-STD-1290 (References 27) but with the velocity, pitch, and roll angles shown in Figure 23. The effort described in Reference 26 utilized both KRASH and NASTRAN analyses for determining the weight increment of the airframe and landing gear for varying levels of crashworthiness.

The systems approach to crashworthiness using KRASH models was applied to a study of two landing gear designs to evaluate their influences on helicopter weights for survivable crash-impact conditions. The results of this study, presented

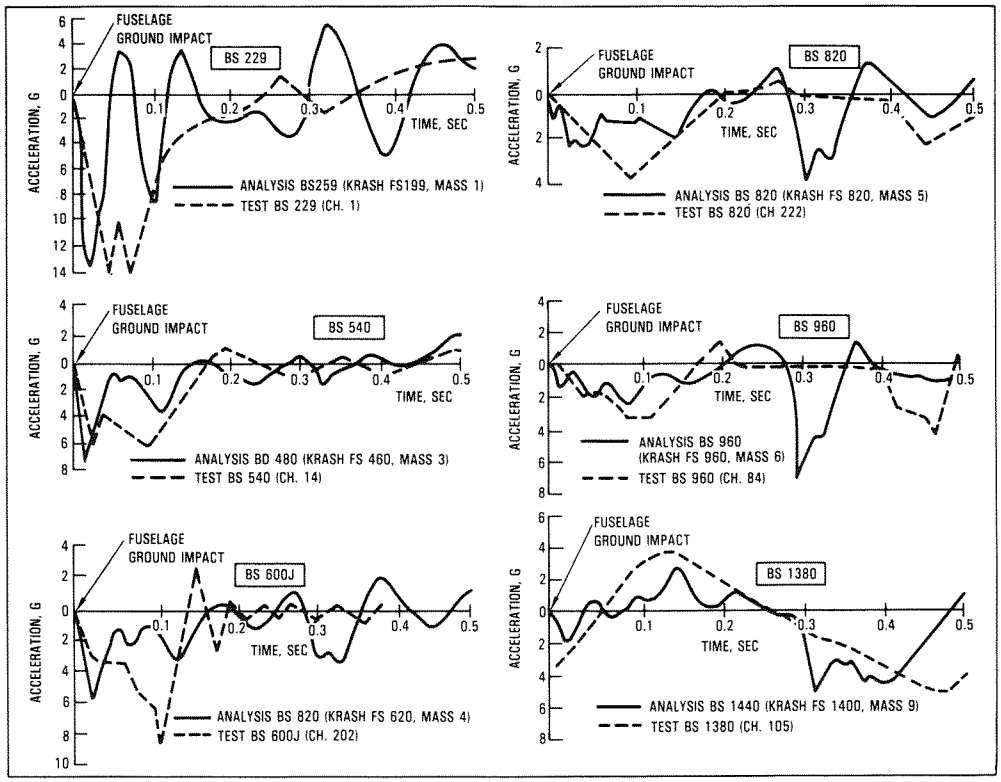


Figure 22. Vertical Acceleration Response, KRASH Versus CID Test Data, Stick Model - Fuselage Ground Impact at 14 ft/sec

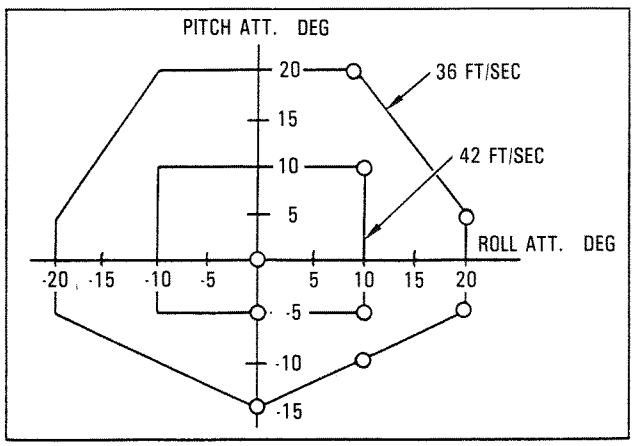


Figure 23. Design Envelope of Vertical Velocity, Pitch, and Roll Attitudes in Crash Impacts for Military Helicopter

in Reference 21, demonstrates how an analytical evaluation of crashworthiness design can be used to assess a weight effective design with respect to both extending the limits of crashworthiness and the cumulative frequency of occurrence of survivable helicopter accidents. Reference 25 presents results of a research objective to design, fabricate, test and fly a composite fuselage which will meet the vertical impact requirements of MIL-STD-1290 with a minimum of 22 percent savings in weight over the existing metal design. The design was evaluated through impact tests and KRASH analyses.

Recently program KRASH was used to develop velocity change and crush distribution envelopes for transport category aircraft. Utilizing full-scale crash test data and the validated KRASH 'CID' model a post-CID parametric study (Reference 17), outlined in Figure 24, was performed. The results of which are shown in Figures 25 and 26.

Composites. A major consideration in the development of crash design criteria is the manner in which designs of composite material in lieu of metals influence dynamic response and load transfer behavior. In the last several years the use of advanced materials, including composites, has accelerated. The biggest strides have been made with military rotorcraft. References 28-34 report on crash analysis of fuselage designs which incorporate composite materials. In all of these studies, program KRASH is the tool with which the analytical study is performed. The purpose of these studies are, generally, to show trade-off between response levels and designs and/or design requirements. These studies point out that; composite materials offer significant benefits over metallic structures in reducing weight and cost as well as improved corrosion resistance. However, composite materials exhibit low strain-to-failure compared to such metals as 2024 aluminum, a ductile metal that can tolerate rather large strains, deform plastically and absorb a considerable amount of energy in the nonlinear region without fracture. Because of this difference between composites and

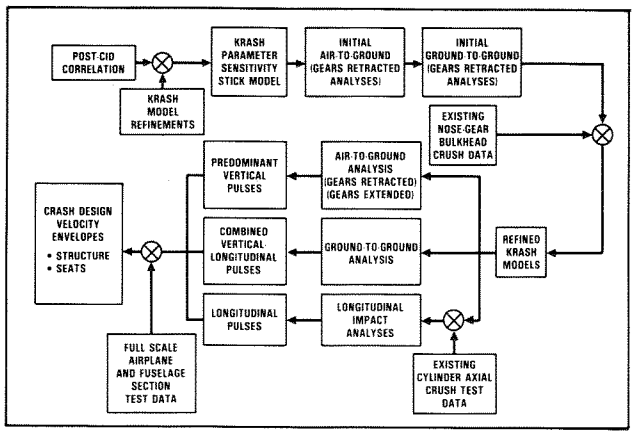


Figure 24. Parameter Sensitivity Analysis Program Flow Diagram

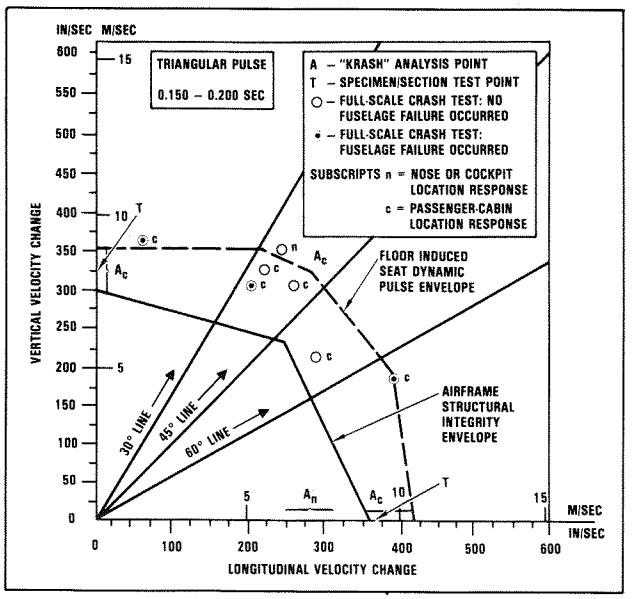


Figure 25. Velocity Envelopes for Transport Category Airplanes

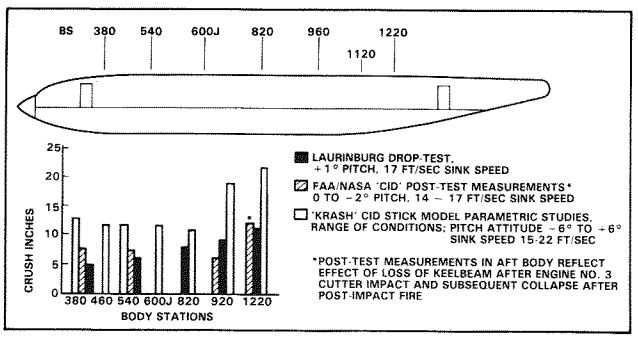


Figure 26. Fuselage Crush

metals, crash energy absorption with composites must come from innovative design to augment the lower material stress-strain behavior of the composites.

Taking into consideration the findings from rotary-wing composites studies, the FAA's approach in the assessment of crash design compatibility of composites in "lieu of" metals is as follows:

1. The energy absorption capability of the structure to be affected by the impact loading must be determined.

   Tests conducted by the FAA Technical Center and supporting analyses, described in Reference 15, illustrate the manner in which current structure can be evaluated so as to establish guidelines for replacement structure. Briefly, this approach consisted of analyzing the structural behavior of a wide-body airplane during a crash impact using program KRASH for specified impact conditions, to determine the response and crushing distribution along the fuselage. This analysis is then followed by a more detailed analysis of the frame segments wherein critical responses can occur. Several section tests and analysis, as sequenced in Figure 27, were performed for this purpose. The FAA conducted two widebody section drop tests. The first consisted of lightly loaded 5000 pounds (2,273 kg) section without cargo (20 ft/sec (6.1 m/sec) impact velocity) and the second of a more densely loaded 10,800 lb (4,909 kg) section with cargo (25 ft/sec (7.62 m/sec) impact velocity). The post-test results shown in Figure 28, vividly demonstrate the crush behavior associated with both specimens. The lightly loaded structure crushed approximately 2 inches (0.05 meters) while the latter crushed as much as 14 inches (0.36 meters). The comparative passenger floor responses are approximately 35g peak acceleration, .040 sec; pulse duration and 16g peak acceleration, .100 sec pulse duration, respectively.

2. The combination of composite material's behavior and designs must exhibit equal or better energy absorption than the metals which they replace. There are several parameters which can be used as measures of performance for comparing composites with metals. The most pertinent parameters are specific energy, which considers energy and weight; load uniformity which indicates the relationship between peak and average force; stroke ratio, which provides a measure of effective use of material; energy dissipation density, which also indicates the degree of effectiveness in absorbing energy; ratio of dynamic to static forces, which reflects a material property such as strain rate which could influence behavior under dynamic loading; and crush stress, which is related to the forces and area involved in the loading. As one could surmise, these parameters can be interrelated.

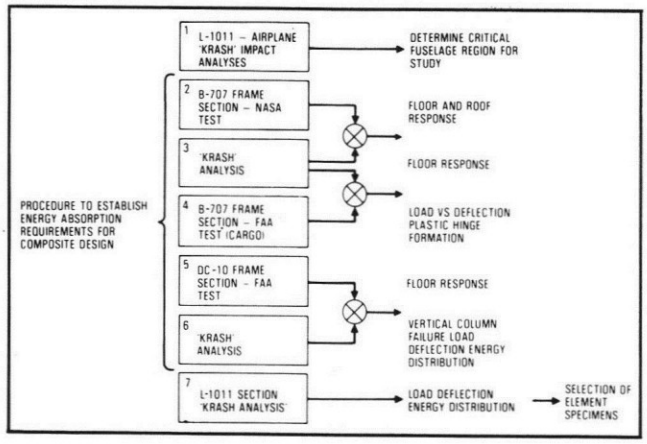


Figure 27. Procedure to Establish Energy Absorption Requirements for Composite Design

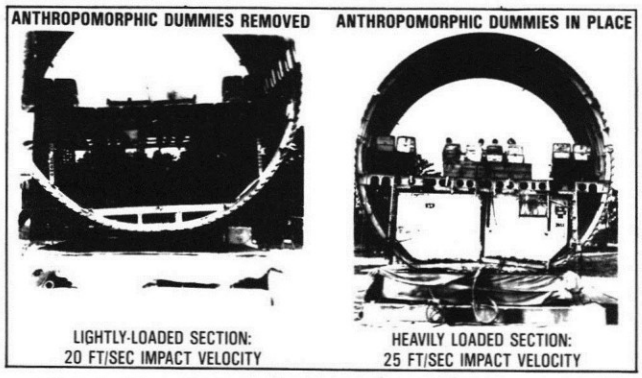


Figure 28. Wide-Body Frame Sections Post-Test Results

3. The failure mode and energy absorption of a composite design must meet design criteria requirements and may not be feasible on a one-to-one substitution basis.

   This premise is borne out by the results from the study described in Reference 32 which illustrated how the details of design with composites can influence results insofar as failure mode and energy absorption are concerned.

Two major domestic helicopter manufacturers recently developed and crash impact tested all composite fuselage designs. Both aircraft were analyzed with program KRASH prior to the impact. In fact the preliminary computer results were used to establish the envelope of survivability and thus helped to select the impact conditions. The test article and results are discussed in Reference 33 and 34. A comparison of the aircraft weights and impact conditions are shown below.

| Aircraft (Ref.) | Weight (lb) | Impact Velocity ft/sec Vertical | Long. | Impact Attitude (deg) Pitch | Roll | Yaw |
|---|---|---|---|---|---|---|
| No. 1 (33) | 7727 | 38.0 | 0.0 | 10.0 | 10.0 | --- |
| No. 2 (34) | 7527 | 41.4 | 26.4 | 15.0 | 14.5 | --- |

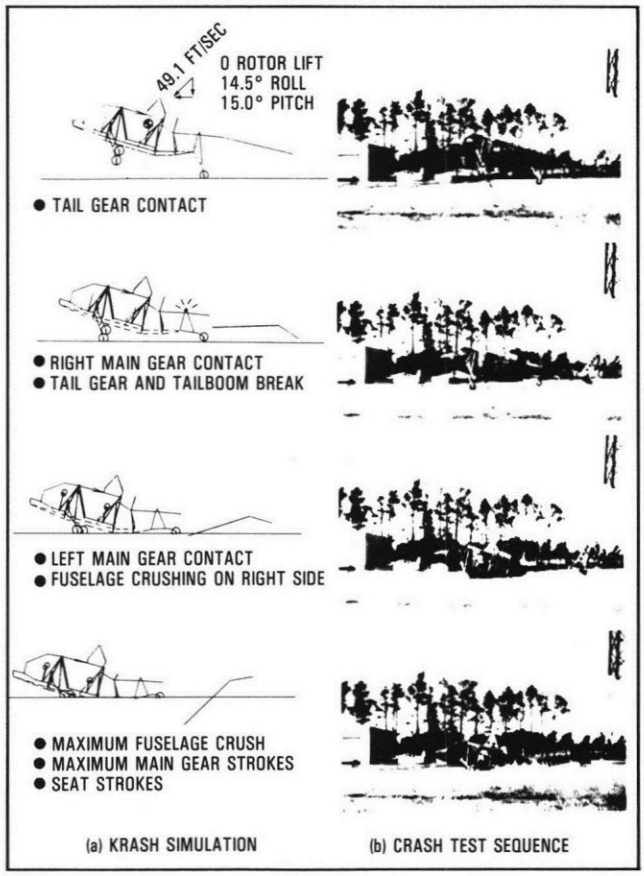


Figure 29. Comparison of KRASH Simulation Versus Test Results

A comparison of the KRASH simulation with the actual event is drawn in Figure 29 from the Reference 34 report. Other data relating the KRASH analysis and crash test events obtained from Reference 34 are shown in Figure 30. Included are (a) comparison of timing of significant events, (b) comparison of vehicle, e.g., vertical velocity time history and (c) distribution of energy absorption during the major impact. The latter is obtained from analysis only and illustrates one of the most important features of KRASH.

## References

1. American Helicopter Society, National Specialist's Meeting on Crashworthy Design of Rotorcraft, Atlanta, Georgia, April 7-9, 1986.

2. Wittlin, G. and Gamon, M. A., "Experimental Program for the Development of Improved Helicopter Structural Crashworthiness Analytical and Design Techniques," USAAMRLDL-TR-72-72, Volumes I and II, May 1973.

3. Wittlin, G. and Gamon, M. A., "Full-Scale Crash Test Experimental Verification of a Method of Analysis for General Aviation Airplane Structural Crashworthiness," FAA Report FAA-RD-77-188, February 1978.

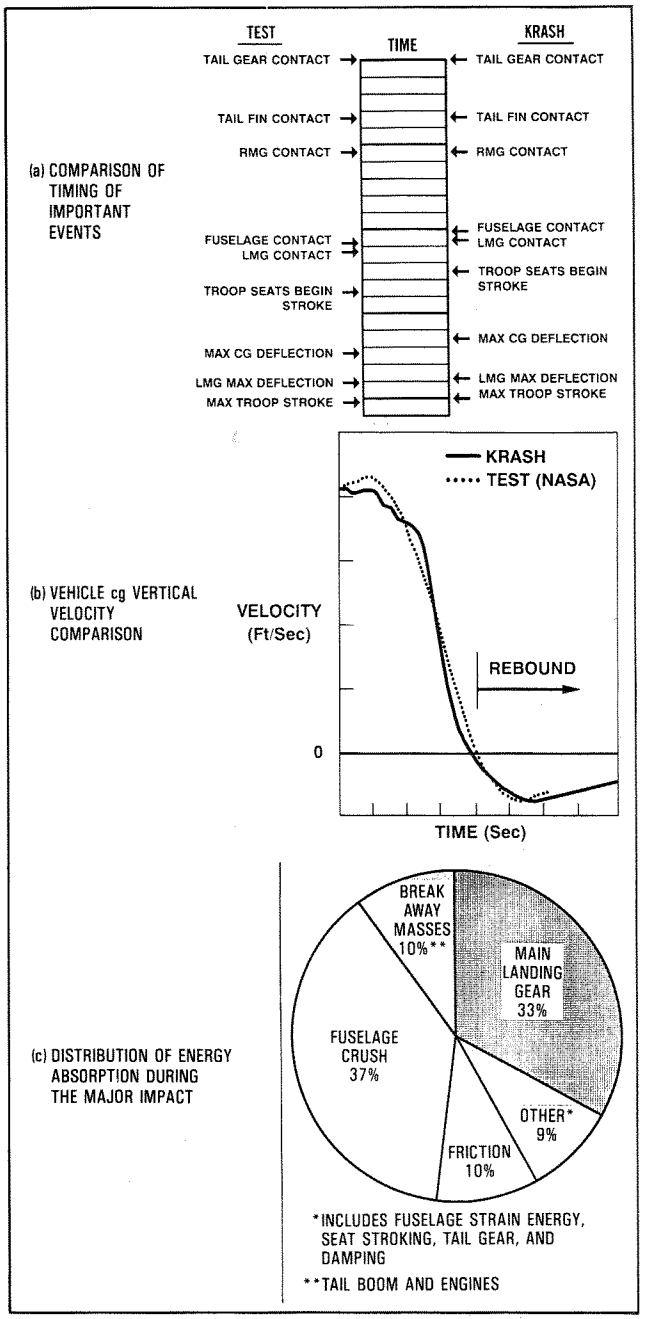


Figure 30. KRASH Analysis Versus Crash Test Events


4. Gamon, M. A., Wittlin, G., and LaBarge, W. L., "KRASH85 User's Guide - Input/Output Format," DOT/FAA/CT-85/10, May 1985.

5. Gamon, M. A., "General Aviation Airplane Structural Crashworthiness User's Manual, Vol. I - Program KRASH Theory." FAA-RD-77-189, February 1978.

6. LaBarge, W. L., "General Aviation Airplane Structural Crashworthiness Programmer's Manual," FAA-RD-78-120 (Revised), June 1979.

7. Widmayer, E., Brende, O., "Commercial Jet Transport Crashworthiness," NASA Contractor Report 165849, FAA Report DOT-FAA-CT-82/86, March 1982.

8. Cominsky, A., "Transport Aircraft Accident Dynamics," NASA Contractor Report 165850, FAA Report No. DOT-FAA-CT-82/70, March 1982.

9. Wittlin, G., Gamon, M. A., Shycoff, D. L., "Transport Aircraft Crash Dynamics," NASA Contractor Report 165851, FAA Report DOT-FAA-CT-82/69, March 1982.

10. Pugliese, S. M., "707 Fuselage Drop Test Report," Report No. 7252-1, Arvin/Calspan Report prepared for the FAA Technical Center, Atlantic City, New Jersey, March 1984.

11. Hayduk, R., Williams, S., "Vertical Drop Test of a Transport Fuselage Section Located Forward of the Wing," NASA TM 85679, National Technical Service, Springfield, Virginia, August 1983.

12. "DC-10 Fuselage Drop Test Report," Report No. 7251-2, Arvin/Calspan report prepared for the FAA Technical Center, Atlantic City, New Jersey, September 1984.

13. Williams, S. A., Hayduk, R. J., "Vertical Drop Test of a Transport Fuselage Center Section Including the Wheel Wells," NASA TM 85706, October 1983.

14. "Full-Scale Transport Controlled Impact Demonstration Program," FAA Report No. DOT/FAA/CT-82/151, FAA Technical Center, Atlantic City Airport, New Jersey, January 1984.

15. Wittlin, G., and LaBarge, W. L., "KRASH Dynamics Analytical Modeling - Transport Airplane Controlled Impact Demonstration Test," DOT/FAA/CT-85/9, May 1985 (Revised March 1986).

16. Wittlin, G., "KRASH Analysis Correlation - Transport Airplane Controlled Impact Demonstration Test," DOT/FAA/CT-86-13, December 1986.

17. Wittlin, G., LaBarge, W. L., "KRASH Parametric Sensitivity Study - Transport Category Airplanes," DOT/FAA/CT-87/13, December 1987.

18. Cronkhite, J. D. and Berry, V. L., "Investigation of the Crash Impact Characteristics of Helicopter Composite Structures," USAAVRADCOM-TR-82-D-14, February 1983.

19. Carnell, B. P., Pramanik, M., "ACAP Crashworthiness Analysis by KRASH," AHS Meeting, March 1983, Philadelphia, Pennsylvania.

20. Sen, J. K., Votaw, M. W., Downer, G. R., "Influence of Two Landing Gear Designs on Helicopter Crashworthiness and Weights," Hughes Helicopters, Inc., AHS Meeting, May 1985, Ft. Worth, Texas.

21. Pramanik, M., "Landing Gear Performance Simulation by KRASH Program," AHS Meeting, April 1986, Atlanta, Georgia.

22. Jackson, A. C., Wittlin, G., Balena, F. J., "Transport Composite Fuselage Technology - Impact Dynamics and Acoustic Transmission" - AFWAL-TR-85-3094, Proceedings of the Seventh Conference on Fibrous Composites in Structural Design, June 1985.

23. Wittlin, G., and Lackey, D., "Analytical Modeling of Transport Aircraft Crash Scenarios to Obtain Floor Pulses," FAA Report DOT/FAA/CT-83/23, NASA CR 1666089, April 1983.

24. Discussions with Dr. M. Sadeghi and Dr. A. Walton, Cranfield Institute of Technology, March 1987.

25. Sen, J. K., Votaw, M. W., "A Skin-Stringer Design for a Crashworthy Composite Fuselage for the Hughes .500E Helicopter," Hughes Helicopters, Inc., AHS Meeting, May 1985, Ft. Worth, Texas.

26. Sen, J. K., et. al., "The Influence of Two Landing Gear Designs on Helicopter Crashworthiness and Weights," AHS Meeting, Ft. Worth, Texas, May 1985.

27. Light Fixed-Wing and Rotary Wing Aircraft Crashworthiness, MIL-STD-1290 (January 1974).

28. Sen, J. K., "Designing for a Crashworthy All-Composite Helicopter Fuselage," AHS, Philadelphia, Pennsylvania, May 1984.

29. Logan, A. H., Votaw, M. W., "The Hughes Integrated Approach to Helicopter Crashworthiness - Past, Present, and Future, AHS, Ft. Worth, Texas, May 1985.

30. Sen, J. K., and Votaw, M. W., "Skin Wing Design for a Crashworthy Composite Fuselage for the Hughes 500E Helicopter," AHS, Ft. Worth, Texas, May 1985.

31. Cronkhite, J. D., "Design of Airframe Structures for Crash Impact," AHS, Atlanta, Georgia, April 1986.

32. Jackson, A. C., et. al., "Transport Composite Fuselage Transmission," NASA CR 4035, December, 1986.

33. Clarke, C. W., "Evolution of the ACAP Crash Energy Management System," presented at the AHS meeting, Washington, D.C., June 16-18, 1988.

34. Cronkhite, J. D., and Mazza, L. T., "Bell ACAP Full-Scale Aircraft Crash Test and KRASH Correlation," presented at the AHS Meeting, Washington, D.C., June 16-18, 1988.